

行政院國家科學委員會專題研究計畫成果報告

克爾效應鎖模雷射之非線性動力學研究

Studies on Nonlinear Dynamics of Kerr-Lens Mode-Locking Lasers

計畫編號：NSC 88-2112-M009-034

執行期限：87年8月1日至88年7月31日

主持人：謝文峰教授 國立交通大學光電工程研究所

一、中文摘要

我們提出在連續非線性微擾下，雷射在共心和共焦腔結構將可能存在超過一個高斯基模同時震盪。在改變克爾鎖模雷射共振腔參數造成的影響研究中發現較對稱共振腔較易形成叉型分岔 (pitchfork bifurcation)，而馬鞍點分岔出現在對稱性破壞時。從分岔的性質我們建議近共焦等臂腔克爾鎖模雷射可望觀察到雷射雙穩態。

關鍵詞：分岔現象、克爾效應和共振腔

Abstract

We propose more than one spatial fundamental Gaussian modes may happen in the concentric and confocal resonators under persisting nonlinear effect. Extensively studying the influence of resonator's parameters in Kerr-lens mode-locked resonator, pitchfork bifurcation results in more symmetrical configurations and saddle-node bifurcation appears as the symmetry being broken. From the properties of bifurcation, we suggest that the equal-arm and near-confocal resonator is suitable for the emergence of bistability in KLM lasers.

Keywords: bifurcation, Kerr effect and resonator

二、緣由與目的

Recently bistability in Kerr-lens mode-locking (KLM) resonators were studied

by many researchers after the KLM laser was built [1-3]. Bistability was firstly predicted in a near-concentric unstable KLM resonator by considering saturable Gaussian gain and Kerr nonlinearity when the pumping rate is modulated about the threshold for laser operation [1]. When both spatial and temporal effects are simultaneously taken into account, the S-shaped bistable behavior of spot size, pulse width and pulse energy with varying pump power was found at a specific near-confocal configuration [2]. In these two researches bistability mainly results from the mixing effect of absorptive (gain saturation) and dispersive (optical Kerr effect) nonlinearity. Excluding gain effect, bistable behavior was also studied in Ref. [3]. By applying the reduced self-focusing ABCD matrix for a Kerr medium and considering the nonlinear coupling of two transversal directions in the elliptical beam, they found more than one TEM₀₀ resonator modes exist near concentric configuration. In the previous results, multiple Gaussian modes are numerically obtained in some specific configurations with the different source of nonlinearity. But, why these configurations are sensitive to nonlinear effect and whether this bistable character is configuration dependent are not given. We will show in this report the bistability depends upon resonator configuration and propose a reasonable illumination from studying dynamics of Gaussian beam propagation.

三、理論預測

In the paraxial approximation, the fundamental propagation of Gaussian beam follows the ABCD law. The q parameter of Gaussian beam is defined as $1/q = 1/R - i\lambda/(\pi w_0^2)$, where R is radius of curvature, w_0 the spot size and λ the wavelength of the beam. After using the q parameter to construct the iterative map, the character of fundamental resonator mode can be determined from the behavior of the map at the period-1 fixed point [4]. Analyzing the stability of the fixed point with the Greene's residue theorem, we obtained the residue in a linear system [4] is

$$\text{Res} = 1 - (2G_1G_2 - 1)^2. \quad (1)$$

Here we had defined $G_1 = a - b/\rho_1$ and $G_2 = d - b/\rho_2$ as the G -parameters for general optical resonators, where ρ_1 and ρ_2 are their radii of curvature for the two end mirrors and $\begin{bmatrix} a & b \\ c & d \end{bmatrix}$ is the transfer matrix of one-way

pass between these two end mirrors. If a fixed point of a map without multiplier $+1$ is isolated, there are no other fixed points within its neighborhood [5]. Contrarily, another periodic orbit could be created or destroyed when the fixed point has a multiplier $+1$. Such saddle-node or pitchfork bifurcation may occur under persisting nonlinear perturbation. Since the system with residue equal to zero has multiplier $+1$ [5], the confocal ($G_1G_2=0$) or concentric ($G_1G_2=1$) configuration could have the above-mentioned bifurcation with the help of Eq.(1). Thus, a general resonator at these configurations has the intrinsic character that may have multiple Gaussian resonator modes under the nonlinear effect.

The nonlinear self-focusing of Gaussian beam in the Kerr medium can be described by using the renormalized q parameter [6]. The

renormalized q parameter will follow the free-space propagation in the Kerr medium with the Kerr parameter K is the cavity beam power over the critical power of self-trapping and the Re and Im represent the real and imaginary parts of a complex number. From self-consistency of q parameters in a resonator, a simple analytical approach was proposed to design the four-mirror folded KLM laser [7]. Since the curvature of Gaussian resonator mode must match those of the end mirrors in lossless system, the curvature of q parameter at output flat mirror M_1 is zero. Thus, we can assume that the q parameter at M_1 is $q_1 = jy = j\pi w^2/\lambda$.

Using the renormalized q parameter concept to transform q_1 through the Kerr medium and the self-consistence at end face II, one can obtain the spot size of fundamental mode at M_1 satisfies a quartic equation of y^2 as [7]

$$h(w, K, \Gamma) = a_4(y^2)^4 + a_3(y^2)^3 + a_2(y^2)^2 + a_1(y^2) + a_0 = 0$$

Here Γ represents a configuration variable that depends on focal length f . The distance between M_1 and M_2 is d_1 , between M_3 and M_4 is d_2 , between M_2 and the end face I of Kerr medium is r_1 and between two curved mirrors is z and the Kerr medium length L , respectively. The coefficients a_4 , a_3 , a_2 , a_1 , and a_0 are functions of K and Γ . Owing to a quartic equation having analytic solutions, one can extensively study the bifurcation behavior of spatial fundamental Gaussian mode in the KLM resonator with various configurations Γ 's and K 's.

四、結果與討論

We will concentrate on the symmetric confocal configuration in the KLM laser which has equal arms with $d_1 = d_2 = 850$ mm and the crystal is placed at the center of two curved mirrors with $r_1 = r_2$. The parameters

of the optical elements referred to the experimental ones [8], in which the radii of curvature of the curved mirrors M_2 and M_3 are both 100 mm and the length of Brewster-cut Ti:sapphire rod is $L=20$ mm. The curved mirrors have been tilted by an angle θ for the astigmatism compensation about Brewster-cut laser rod. Thus, the resonator could be divided into two astigmatic optical systems associated with the sagittal and tangential planes. These two planes are considered to be orthogonal. Because the similar behavior can also be found in both planes, we focused the following numerical simulation on the sagittal plane. Since the beam's q-parameter contains only the spot size with zero curvature at the output mirror M_1 , the spot size is chosen as the scalar measure in the numerical simulation. The Kerr parameter offers the nonlinear effect to be the bifurcation parameter.

Fig. 1(a) shows spot size at M_1 versus Kerr parameter for $z = 115.3\text{mm}$, $r_1 = r_2 = 47.65\text{mm}$ and $\theta = 14.5^\circ$ in the symmetrical stable resonator. The solid line in this figure indicates the stable solutions of self-consistent Gaussian beam and the dashed line represents the unstable one. The configuration is near confocal, since the confocal configuration for linear (cw) resonator corresponds to a separation of the curved mirrors $z_c=115.267\text{mm}$. As predicted in the previous section, the bifurcation appears as a pitchfork bifurcation with the bifurcation point at $(K_b, w_b) = (0.04278, 0.4513 \text{ mm})$, where K_b and w_b represent the critical bifurcation Kerr parameter and spot size. Furthermore, we numerically obtain $h = h_w = h_{ww} = h_K = 0$ at the bifurcation point, where the subscripts of function $h(w, K, L)$ represent the various order partial derivatives with respect to the

variables indicated as the subscripts. According to the singularity theory [9], this result also verifies that the classification belongs to the pitchfork bifurcation.

When the crystal is located away the center of two curved mirrors, the characteristics of bifurcation will be changed. By constraining $z=115.3$ mm, the bifurcation diagram with $r_1=46.5\text{mm}$ is shown in Fig. 1(b), note that $r_1=47.65$ mm for symmetry resonator. It is no longer a standard pitchfork bifurcation but a perturbed one. Owing to pitchfork bifurcation is not generic, it usually results from some peculiar symmetry or the inadequacy of the idealization, in which some small effects are neglected [9]. Therefore, moving the crystal away the center of two curved mirrors had broken the symmetry and induced the perturbed variation of bifurcation. In Fig. 1(b), the upper branch of this typical perturbed bifurcation corresponds to the continuous evolution branch from before to after bifurcation. On the contrary, the other typical perturbed pitchfork bifurcation takes place at r_1 greater than 47.65 mm. For example $r_1=49$ mm in Fig. 1(c), the lower branch in this type is a continuous evolution one.

When a slit is inserted at M_1 in a hard aperturing KLM resonator, the KLM strength δ is determined by the rate of change of the spot size as increasing the laser power [7,10]. Experimentally for achieving the larger self-amplitude modulation, in general the slit is inserted vertical to the tangential plane, in which has the larger KLM strength. If the configuration has the pitchfork bifurcation in the sagittal plane with $\delta < 0$ in the tangential plane, it is suitable for observing the bistability in hard-aperturing KLM laser. Under well matching the astigmatism, δ has the same sign in both

planes, thus the configuration with the type like $r_1=49$ mm in Fig. 1(c) prefers to operate at KLM due to $\delta < 0$ in both planes. Whereas, the configuration with the type like $r_1=46.5$ mm in Fig. 1(b) will not be a preferable KLM one.

If we considering the asymmetric resonator with $d_1 \neq d_2$ but $d_1+d_2=170$ cm, the different classification of bifurcation will take place. In Fig. 2 with $d_1=70$ cm, $d_2=100$ cm, $z=114.74$ mm and $r_1=41$ mm, saddle-node bifurcation occurs at critical bifurcation parameter $K_b \approx 0.08993$. There are no real solution of spot size as $K < K_b$, and two self-consistent spot sizes exist as $K > K_b$. The lower branch with solid line indicates stable solutions and the upper branch with dashed line represents unstable solutions. When the configuration varies close to the confocal one, the K_b decreases. In general, pitchfork bifurcation will occur in more symmetrical configurations and saddle-node bifurcation exists as this symmetry being broken [5]. Therefore, we think the emergence of different classification mainly results from the configurations having the unequal arms, which have broken the symmetry of resonator.

However, the symmetry broken from the slightly unequal arms can be compensated by the tilted angle θ of the curved mirrors. The critical bifurcation parameter against the tilted angle is shown in Fig. 3 with $d_1 = 83$ cm, $d_2 = 87$ cm, $z = 115$ mm and $r_1 = 40$ mm which corresponds to near-confocal configuration. We constrain our discussions on $K_b < 0.4$ that the associated power can be obtained from general experiments. As $\theta < \theta_a = 13.7709^\circ$, the configuration has only one real solution of spot size and no bifurcation. Increasing the tilted angle to $\theta > \theta_a$, we find the saddle-node bifurcation takes place. The upper branch corresponds

to the stable solution and the lower branch corresponds to the unstable solution. Moreover, K_b increases as increasing the tilted angle, but the stability reverses and the K_b decreases as increasing the tilted angle to $\theta > \theta_b = 13.9155^\circ$. When θ is greater than $\theta_c = 14.1207^\circ$, the bifurcation transits to the perturbed pitchfork bifurcation and K_b still decreases as increasing θ . The minimum K_b is 0.04955 at $\theta_a = 14.1361^\circ$ corresponding to the standard pitchfork bifurcation. The other type of perturbed pitchfork bifurcation exists as $\theta_a < \theta < \theta_b = 14.2186^\circ$, in which K_b increases as increasing θ . The configuration returns to having one reasonable spot size as $\theta > \theta_b$ if one constrains $K_b < 0.4$. In fact, dynamical characteristics in this region still belongs to the pitchfork bifurcation for $K_b > 0.4$. Because such a K value is not easy to reach in general KLM lasers, the phenomenon of bifurcation may not be observed in experiments. It is note that the above regions all have $\delta < 0$ in tangential plane, i.e., these regions prefer to KLM operation with hard aperture. Although the tilted angle can compensate the broken symmetry resulting from unequal arms, the latter one governs the emergence of bifurcation. If we constrain $d_1 + d_2 = 170$ cm and $d_1 \leq d_2$, the region of pitchfork bifurcation is about hundreds of μm for z translation in equal-arm resonator. The region quickly shrinks as increasing $|d_1 - d_2|$ and becomes less than $10\mu\text{m}$ as $|d_1 - d_2| \geq 4$ cm even having the tilted angle compensation.

The bifurcation phenomenon can also be found in the near-concentric resonator. But the region having bifurcation is smaller than that of near-confocal resonator, and its classification belongs to the saddle-node bifurcation. Since saddle-node bifurcation has only one stable solution, bistability will not be found in such configuration if we just

consider the self-focusing effect. Moreover, no steady spot size in the range with $K < K_t$, represents that the resonator lacks a steady pulse generating mechanism from cw with $K = 0$ transiting to KLM with higher K . This system may not be spontaneous in KLM laser. On the contrary, bistability could be observed in the configuration with unperturbed or perturbed pitchfork bifurcation having two stable spot sizes in $K > K_t$ and a steady one in $K < K_t$; especially, the configurations having $\delta < 0$ in tangential plane is achievable to mode-locking operation with hard aperture. Thus, we suggest that the equal-arm and near-confocal resonator is suitable for the emergence of bistability in experiment due to the region with pitchfork bifurcation being large.

When we further consider the spatial and temporal effects in a KLM resonator, a simple quadratic equation is obtained to determine the pulse width from space-time analogy [12]. Owing to the spot size variation in Kerr medium couples to temporal self-phase modulation matrix, the bifurcation of spot size will result in the bifurcation of pulse width. We indeed found the same classification of bifurcation in pulse width versus Kerr parameter. It is also found in Ref. [2] that both spot size and pulse width appears the same bistability behavior. But S-shaped behavior in Ref. [2] is not found and instead of pitchfork bifurcation in this research, this difference may be attributed to the gain saturation effect.

五、結論

Studying the iterative map constructed from the propagation of Gaussian q parameter in a resonator, we found that the confocal and concentric configuration corresponding to the map having multiplier $+1$. Such a map will induce bifurcation

under nonlinear perturbation in general. This result gives a reasonable interpretation for the existence of multiple fundamental Gaussian modes, which often occur at the limit of stable region. When the numerical simulations contain only the self-focusing and ignore the gain saturation effect in KLM resonator, bistability takes place in the above-mentioned configurations. Under extensively studying the influence of different arm-lengths, crystal position and tilted angle, there are two main classification bifurcation corresponding to pitchfork and saddle-node ones. Pitchfork bifurcation occurs in configurations with higher symmetry and saddle-node bifurcation exists as this symmetry being broken. In addition, we suggest that the equal-arm and near-confocal resonator is suitable for the emergence of bistability in experiment.

六、自我評估

在理論上我們完成探討近共焦、以及低階共振結構的動力學研究，並完成對應的實驗成果，包含週期二、週期三、和轉變成渾沌之路徑，正在整理撰稿中。另外，我們也以簡單端幫雙鏡 Nd:YVO₄ 固態雷射研究這些特殊結構之雷射模態，發現超低閾值和光腰縮小之現象 (Optics Commun. 1999)，和首次發現此現象可能是此雷射操作在多光程共振模之故。此成果已完成撰稿。因此本年度之成果還算豐碩。

七、參考文獻

1. M. Piché, Opt. Commun. 86 (1991) 156.
2. S. Longhi, Opt. Commun. 110 (1994) 120.
3. R. E. Bridges, R. W. Boyd, and G. P. Agrawal, Opt. Lett. 18 (1993) 2026.
4. M.-D. Wei, W.-F. Hsieh, and C. C. Sung, Opt. Commun. 146 (1998) 201.
5. R. S. MacKay, Renormalisation in Area-preserving Maps, (World Scientific, Singapore, 1993).

6. H. A. Haus, J. G. Fujimoto, and E. P. Ippen, IEEE J. Quantum Electron. 28 (1992) 2086.
7. K.-H. Lin and W.-F. Hsieh, J. Opt. Soc. Am. B. 11 (1994) 737.
8. D.-G. Juang, Y.-C. Chen, S.-H. Hsu, K.-H. Lin, and W.-F. Hsieh, J. Opt. Soc. Am. B, 14 (1997) 2116.
9. R. Seysel, Practical Bifurcation and Stability Analysis, (Springer-Verlag, New York, 1994) Chapter 8.
10. G. Cerullo, S. De Silvestri, and V. Magni, Opt. Lett. 19 (1994) 1040.
11. M.-D. Wei, W.-F. Hsieh, and C. C. Sung, Opt. Commun. 155 (1998) 406.
12. K.-H. Lin and W.-F. Hsieh, J. Opt. Soc. Am. B. 13 (1996) 1786.

line for stable solutions and dashed line for unstable one.

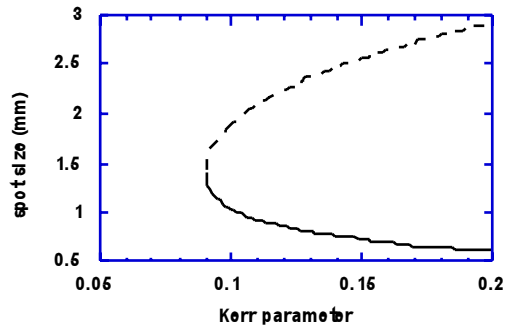


Fig. 2 Saddle-node bifurcation at $d_1=700$, $d_2=1000$, $z=114.74$ and $r_1=41$ mm, respectively.

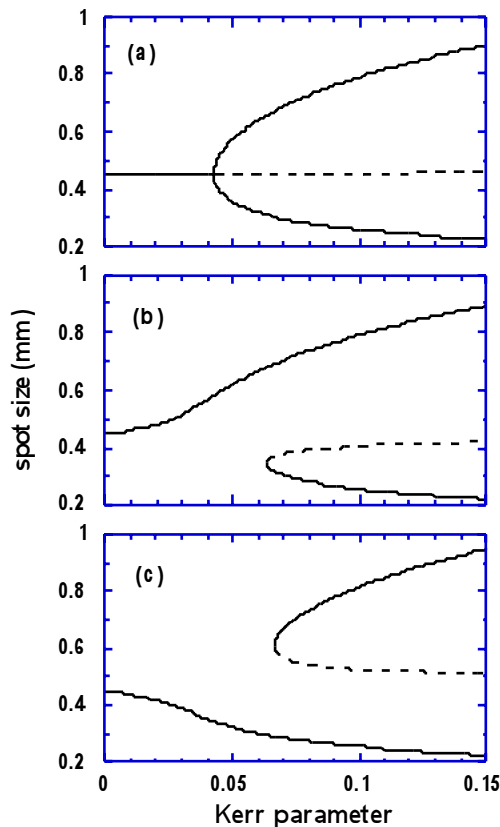


Fig. 1 Pitchfork bifurcation. The spot size versus Kerr parameter with $d_1 = d_2 = 85$ cm is shown for $z = 115.3$ mm and (a) $r_1=47.65$ mm, (b) $r_1=46.5$ mm and (c) $r_1=49$ mm. The solid

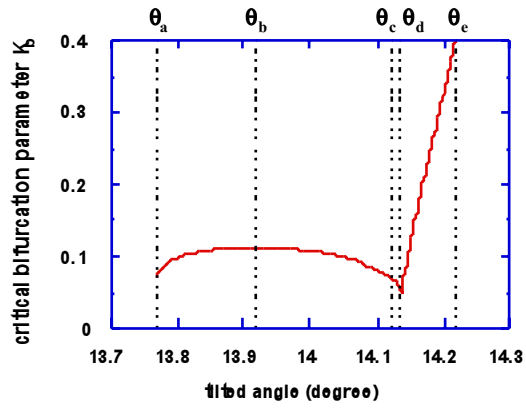


Fig. 3 The critical bifurcation parameter versus tilted angle with $d_1=830$, $d_2=870$, $z=115$ and $r_1=40$ mm, respectively.